

Technical University of Denmark



Factors affecting the hydraulic performance of infiltration based SUDS in clay

Bockhorn, B.; Klint, K.E.S.; Locatelli, Luca; Park, Y.; Binning, Philip John; Sudicky, E.; Jensen, Marina Bergen

Published in:
Urban Water Journal

Link to article, DOI:
[10.1080/1573062X.2015.1076860](https://doi.org/10.1080/1573062X.2015.1076860)

Publication date:
2017

Document Version
Peer reviewed version

[Link back to DTU Orbit](#)

Citation (APA):
Bockhorn, B., Klint, K. E. S., Locatelli, L., Park, Y., Binning, P. J., Sudicky, E., & Jensen, M. B. (2017). Factors affecting the hydraulic performance of infiltration based SUDS in clay. *Urban Water Journal*, 14(2), 125-133.
DOI: 10.1080/1573062X.2015.1076860

DTU Library

Technical Information Center of Denmark

General rights

Copyright and moral rights for the publications made accessible in the public portal are retained by the authors and/or other copyright owners and it is a condition of accessing publications that users recognise and abide by the legal requirements associated with these rights.

- Users may download and print one copy of any publication from the public portal for the purpose of private study or research.
- You may not further distribute the material or use it for any profit-making activity or commercial gain
- You may freely distribute the URL identifying the publication in the public portal

If you believe that this document breaches copyright please contact us providing details, and we will remove access to the work immediately and investigate your claim.

Factors affecting the hydraulic performance of infiltration based SUDS in clay

Abstract

The influence of small scale soil heterogeneity on the hydraulic performance of infiltration based SUDS was studied using field data from a clayey glacial till and groundwater simulations with the integrated surface water and groundwater model HydroGeoSphere. Simulations of homogeneous soil blocks with hydraulic properties ranging from sand to clay showed that infiltration capacities vary greatly for the different soil types observed in glacial till. The inclusion of heterogeneities dramatically increased infiltration volume by a factor of 22 for a soil with structural changes above and below the CaCO_3 boundary. Infiltration increased further by 8% if tectonic fractures were included and by another 61% if earthworm burrows were added. Comparison of HydroGeoSphere infiltration hydrographs with a simple soakaway model (Roldin et al. 2012) showed similar results for homogenous soils but indicated that exclusion of small scale soil physical features may greatly underestimate hydraulic performance of infiltration based SUDS.

Keywords

Infiltration; Stormwater modelling; SUDS

19 **1 Introduction**

20 Sustainable urban drainage systems (SUDS), also referred to as Water Sensitive Urban Design
21 (WSUD), are used to mimic the natural water balance, often through stormwater infiltration into the
22 soil. Infiltration based SUDS have various forms: rain gardens or infiltration basins collect
23 stormwater directly at the surface or very close to it; whereas soakaways, or infiltration trenches,
24 infiltrate stormwater underground (e.g. Hoyer et al. 2011, Freni et al. 2004). The utilization of the
25 device allows for both quantitative and qualitative control of stormwater runoff during and after rain
26 events and their design is based on inflow, outflow and detention water volumes (Freni et al. 2009,
27 Campisano et al. 2011, Creaco and Franchini 2012). The efficiency of an infiltration device is
28 dependent on the hydraulic properties of the surrounding soil.

29 Many soils in the Northern Hemisphere are derived from deposits of the last Weichselian glaciation
30 (Houmark-Nielsen 1999). Though they generally have a high clay content and low matrix
31 permeability, they are highly heterogeneous with hydraulic conductivities varying by several orders
32 of magnitude (Fredericia 1990, Klint 2001, Nilson 2001).

33 Infiltration capacities also vary with depth due to changes in soil structure. Macropores like
34 fractures, root holes and earthworm burrows have a major effect on infiltration, especially in low
35 permeable soils (Klint and Gravesen 1999). For example, anecic earthworm species increase
36 infiltration rates since they create semi-permanent to permanent vertical burrows into deep soil
37 layers (Edwards 2004, Lee 1985). Root holes can also serve as important pathways for water flow
38 in soils (Jarvis 2007) and have been studied by many authors. Meek et al. (1989) observed increased
39 ponded infiltration rates by a factor of 2-3 under a 3-year old alfalfa stand compared to loose soil.
40 Root holes are therefore likely to lead to increased infiltration rates in SUDS located in vegetated
41 infiltration settings. In addition vegetation improves conditions for earthworms by increasing the C
42 and N content in the soil (Smetak et al. 2011). Earthworm burrows often have a direct connection to
43 the surface and a greater aperture than fractures and so have a greater effect on enhanced
44 stormwater infiltration than fractures which usually start at greater depths. Macropores become
45 hydraulically active in wet soil when the soil matric potential exceeds the macropores entry
46 potential, but they do not conduct water in relatively dry soil, so that they can, depending on the
47 degree of saturation, either serve as pathways for rapid downward movement of water or function as
48 capillary barriers in the vadose zone (Wang and Narasimhan 1985). Preferential flow patterns can
49 be identified with the help of dye tracer experiments (Jørgensen et al. 2002).

50 The CaCO₃ boundary usually lies in the upper 1.3 to 2.0 meters of the tills, with CaCO₃-free
51 conditions above the boundary and CaCO₃-rich conditions below. The CaCO₃-free soil layers
52 usually have a higher permeability and matrix porosities than the soil layers below, both due to the
53 dissolution of CaCO₃ and the presence of densely spaced and randomly orientated desiccation
54 fractures (Klint and Gravesen 1999, Rosenbom et al. 2009).

55 Methods are available to account for soil heterogeneity in models in order to simulate the
56 performance of stormwater infiltration based SUDS (e.g. Roldin et al. 2012) but their performance
57 is dependent on the accuracy of the input data and often hydrogeological models lack sufficient
58 geological information (e.g. Hansen et al. 2013). Sophisticated hydrological processes such as
59 macropore flow have not previously been incorporated into stormwater models (Elliott and
60 Trowsdale 2007). However, since macropores are ubiquitous features in many types of sediments, it
61 is important to include their characteristics in models if we wish to predict the hydraulic
62 performance of infiltration based SUDS.

63 While root holes have not yet been included in models, empirical studies of rain gardens have
64 shown increased infiltration around root holes compared to bare soils. These root holes have proven
65 to be effective to prevent clogging of rain gardens from debris input (Virahsawmy et al. 2014).

66 Observations of infiltration based SUDS have shown that their hydraulic performance often differs
67 from model predictions, for example infiltration capacities of rain gardens are often underestimated
68 which results in oversizing (Backhaus and Fryd 2013). Soakaways have been shown to have high
69 failure rates due to poor maintenance, inappropriate siting or high debris input (Woods-Ballard et al.
70 2007).

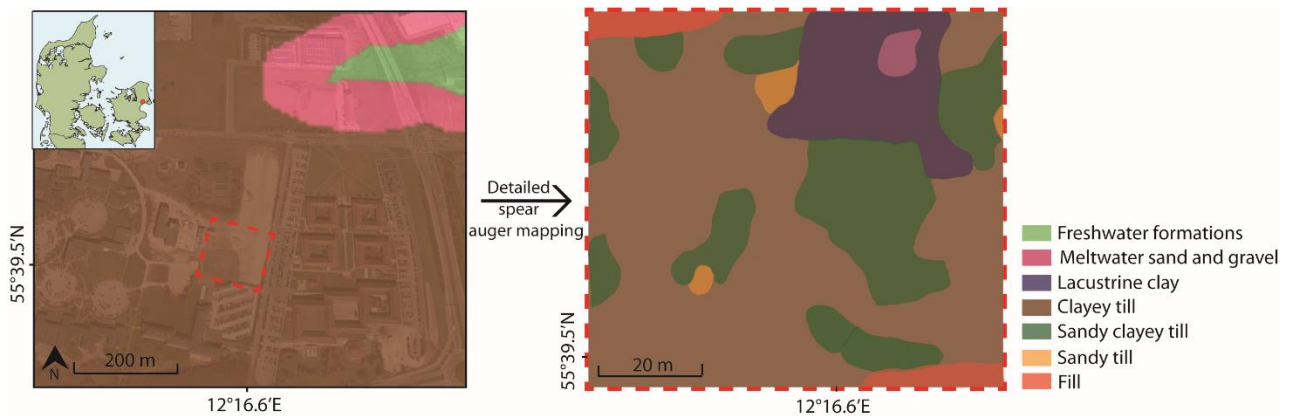
71 Fractures and biopores are ubiquitous in soils. This study aims to show that these small scale
72 geological features have a significant effect on infiltration capacities, and should be considered
73 when positioning and sizing infiltration based SUDS. The paper focuses on clayey tills and the
74 effect on infiltration rates of small scale features like CaCO₃ poor and rich soil layers, earthworm
75 burrows and tectonic fractures. Geological data characterizing a clayey till were employed with the
76 discrete fracture model HydroGeoSphere (Therrien et al. 2009, Aquanty Inc. 2013) in simulations
77 of variably saturated flow. Infiltration rates of four different homogenous soils were in a first step
78 compared to infiltration rates produced with a simple soakaway model by Roldin et al. (2012) to
79 investigate whether the soakaway model works well for homogeneous conditions. In a second step

80 infiltration rates of the homogenous soils were compared to infiltration rates obtained in structured,
81 macroporous soils. Based on the findings this paper discusses implications for maintenance and
82 siting of infiltration based SUDS.

83

84 **2 Study area**

85 To illustrate the importance of soil heterogeneity for SUDS performance data was obtained
86 from a study area situated on an undulating till plain dominated by primarily basal sandy and
87 clayey till, located approximately 20 km west of Copenhagen in Denmark. The site is
88 representative for many formerly glaciated areas of the Northern Hemisphere. In a previous
89 study Bockhorn et al. (2014) refined a geological map of the area on scales 200 m x 200 m
90 using spear auger mapping to scales of 5 m x 5 m / 10 m x 10 m at a 0.8-1.0 m depth.
91 Sediments samples ranged from sandy tills to lacustrine postglacial clays in a depression
92 (Figure 1). The study area is surrounded by houses, parking lots and roads and therefore
93 represents a common urban setting.



94

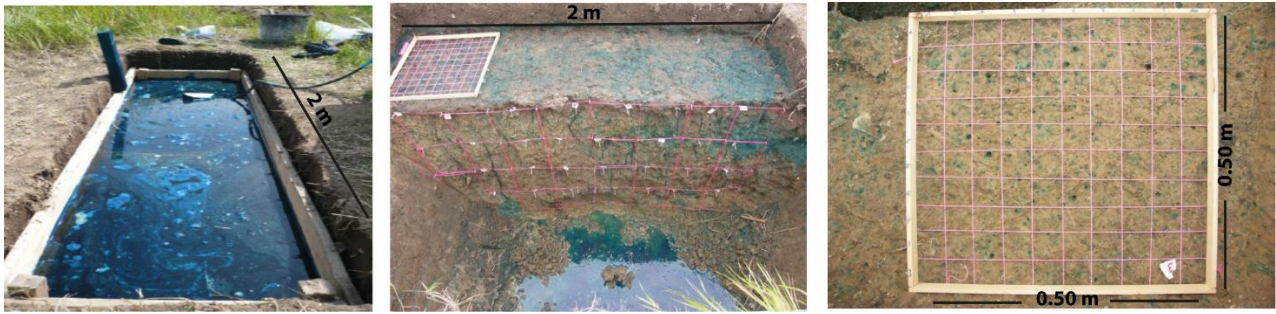
95 Figure 1. Study area on a traditional geological map with 200 m by 200 m resolution (left).
96 Same area after refining with spear auger mapping with grid-sizes 5 – 10 m (right). Study area
97 marked with red dotted line.

98 **3 Material and Methods**

99 **3.1 Tracer test**

100 To characterize the properties of local small scale soil physical features and to determine the
101 macropore distribution, a tracer experiment was carried out in May 2012. The observed macropore
102 distribution is incorporated into the modeling simulations for a realistic prediction of infiltration

103 behavior. Brilliant Blue was used as a tracer and applied to a 2.0 m x 0.5 m area. Before tracer
 104 application, the grass covered top soil was carefully removed to approximately 30 cm depth and a
 105 vacuum cleaner was used to clean the exposed surface to avoid smearing and clogging of the
 106 macropores by loose sediment. The trench was stabilized with a wooden frame and covered with
 107 gravel. Tap water was infiltrated over a period of several hours until saturated conditions in the soil
 108 column under the trench were achieved, and then the tracer was applied (20 l of Brilliant Blue
 109 solution), so that the dye only migrates into hydraulic active macropores. The trench was covered
 110 with a tarpaulin to minimize disturbance by outside factors. Four days after tracer application the
 111 site was excavated to a depth of 150 cm, corresponding to the location of the water table. The
 112 density of the dyed fractures was measured along vertical and horizontal scan-lines at 25 cm
 113 intervals on a vertical wall of the excavation pit. The density of dyed earthworm burrows was
 114 determined on horizontal planes at 25 cm depth intervals (Figure 2). The CaCO₃ boundary was
 115 determined by addition of 10% HCl.



116
 117 Figure 2. Left: set-up of tracer experiment to determine fracture and earthworm burrow distribution.
 118 Middle: exposure of vertical wall four days after tracer application for macropore analysis. Right:
 119 counting of earthworm burrows with the help of a 5 cm x 5 cm grid in a wooden frame.

120 3.2 Model simulations

121 This study employed HydroGeoSphere which is a three-dimensional control-volume finite element
 122 model that simulates surface water flow and unsaturated flow in discretely fractured or non-
 123 fractured porous media. Unsaturated flow is simulated by a modified form of Richards' Equation:

$$124 \quad -\nabla \left(-\bar{K} \cdot k_r \nabla (\psi + z) \right) + [ex \pm Q = \frac{\partial}{\partial t} (\theta_s S_w) \quad (1)$$

125 where \bar{K} is the hydraulic conductivity tensor, k_r is the relative permeability, ψ is the pressure head, z
 126 is the elevation head, $[ex$ is the subsurface fluid exchange rate with the surface domain, Q is a
 127 subsurface fluid source or sink, θ_s is the saturated water content, and S_w is the water saturation.

128 Fracture flow is simulated in two dimensions and a common node approach is used to couple flow
 129 in the fractures and matrix, based on the assumption of continuity of hydraulic head between the
 130 two domains. Flow velocities in the fractures are determined by the cubic law (Witherspoon et al.
 131 1980). Retention and relative permeability for both fractures and porous media are given by van
 132 Genuchten functions or in a table form. For seamless integration of surface and subsurface flow, the
 133 porous medium is coupled with an overland domain and surface flow is described by the diffusion-
 134 wave approximation of the Saint Venant equations:

$$135 \quad \frac{\partial \phi_0}{\partial t} + \frac{\partial(\bar{v}_x \phi_0 d_0)}{\partial x} + \frac{\partial(\bar{v}_y \phi_0 d_0)}{\partial y} + d_0 [I_0 \pm Q_0] = 0 \quad (2)$$

136 where ϕ_0 is the surface porosity, \bar{v}_{x_0} and \bar{v}_{y_0} are the vertically averaged flow velocity in the x and y
 137 directions, respectively, d_0 is the water depths, $[I_0$ is the fluid exchange rate with the subsurface, and
 138 Q_0 is a surface fluid source or sink (Therrien et al. 2009).

139 The infiltration rates and emptying times simulated by HydroGeoSphere were compared to those
 140 obtained by the simple soakaway model presented by Roldin et al. (2012). The model of Roldin et
 141 al. (2012) is based on the soakaway mass balance:

$$142 \quad n \cdot l \cdot w \cdot \frac{dh}{dt} = Q_{in} - Q_{out} \quad (3)$$

143 where n is the porosity of the soakaway filling material, l is the length of the soakaway, w is the
 144 width of the soakaway, h is the water level in the soakaway, t is the time and Q_{in} and Q_{out} are the
 145 inflow and outflow rates from the soakaway. Q_{out} is the sum of the overflow rate and the infiltration
 146 rate. The infiltration rate f is assumed to be equal to the product between the hydraulic conductivity
 147 and the wetted area of the soakaway:

$$148 \quad f = klw + k2h(l + w) \quad (4)$$

149 where k is the soil hydraulic conductivity and klw represents the infiltration from the bottom of the
 150 soakaway whereas $k2h(l+w)$ the infiltration from the sides. The storage volume is described as
 151 $V=lwd/n$, where d is the height of the soakaway and n is the porosity of the filling material.

152 The same soil physical parameters were employed as were used in the HydroGeoSphere
153 simulations, and the infiltration rates and difference in soakaway emptying time compared for the 2
154 models.

155

156 **3.3 Model domains**

157 To assess the variability of the infiltration capacity at the site, four 150 cm thick homogenous
158 domains were set up to reflect the most dominant soil types sampled at the site Soil physical
159 parameters were used to determine retention function parameters using the data provided by Carsel
160 and Parrish (1988) (see Table 1). The same parameters were used in the soakaway models of Roldin
161 et al. (2013).

162

163 The weighted mean for K_{sat} was determined by weighting each individual soil type by the size of
164 the area covered.

165 Based on the information gained from the geological description of the excavation and the tracer
166 test, the model was refined by adding additional soil physical features to the model domain, in the
167 following sequence CaCO_3 , fractures, earthworm burrows. The macropore distribution from the 1
168 m^2 large excavation pit was downsized to the 40.4 cm^2 large model area. The homogenous clayey
169 till is the dominant sediment type on the study area and so was used for the base scenario.

170 In the heterogeneous simulations, the model was subdivided into two distinct layers (above and
171 below CaCO_3 boundary). Randomly oriented desiccation fractures occur in the zone above the
172 CaCO_3 boundary and were included in the model by embedding them into the matrix using the
173 method proposed by Rosenbom et al. (2009). Tectonic fractures and earthworm burrows were
174 added to the domain, with the distribution of macropores being taken from the results of the field
175 investigation. All other parameters were obtained from the study of Rosenbom et al. (2009) (Table
176 1).

177

178 Table 1. Model input parameters used in HydroGeoSphere simulations. Parameters for sandy till,
 179 clayey till, sandy clayey till and lacustrine clay were obtained from Carsel and Parrish (1988)
 180 ('loamy sand', 'clay', 'sandy clay loam' and 'silty clay'). Parameters for soil layer 'above CaCO₃-
 181 boundary' and 'below CaCO₃-boundary', and macropore parameters were obtained from Rosenbom
 182 et al. (2009).

Medium	Parameter	Value	Medium	Parameter	Value
Sandy till (<i>'loamy sand'</i>)	K _{sat} [cm/min]	0.243054	Clayey till (<i>'clay'</i>)	K _{sat} [cm/min]	0.0033
	Porosity [cm ³ cm ⁻³]	0.41		Porosity [cm ³ cm ⁻³]	0.38
	Residual saturation [cm ³ cm ⁻³]	0.057		Residual saturation [cm ³ cm ⁻³]	0.068
	Van Genuchten Paramter:			Van Genuchten Paramter:	
	Alpha [1/cm]	0.124		Alpha	0.0088
	Beta	2.28		Beta	1.09
Sandy clayey till (<i>'sandy clay loam'</i>)	K _{sat} [cm/min]	0.02183	Lacustrine clay (<i>'silty clay'</i>)	K _{sat} [cm/min]	0.000333
	Porosity [cm ³ cm ⁻³]	0.39		Porosity [cm ³ cm ⁻³]	0.36
	Residual saturation [cm ³ cm ⁻³]	0.1		Residual saturation [cm ³ cm ⁻³]	0.070
	Van Genuchten Paramter:			Van Genuchten Paramter:	
	Alpha	0.059		Alpha	0.005
	Beta	1.48		Beta	1.09
Above CaCO₃ boundary	K _{sat} [cm/min]	0.324	Tectonic fractures	Aperture [cm]	0.01
	Porosity [cm ³ cm ⁻³]	0.36		Residual saturation [cm ³ cm ⁻³]	0.01
	Residual saturation [cm ³ cm ⁻³]	0.08		Van Genuchten Paramter:	
	Van Genuchten Paramter:			Alpha	0.04687
	Alpha	0.00698		Beta	2.29719
	Beta	2.0			
Below CaCO₃ boundary	K _{sat} [cm/min]	0.000108	Earthworm burrows	Aperture [cm]	0.4
	Porosity [cm ³ cm ⁻³]	0.31		Residual saturation [cm ³ cm ⁻³]	0.01
	Residual saturation [cm ³ cm ⁻³]	0.007		Van Genuchten Paramter:	
	Van Genuchten Paramter:			Alpha	0.1
	Alpha	0.00293		Beta	2.0
	Beta	1.07442			

183 **3.4 Mesh and Boundary conditions**

184 The same boundary conditions were used for all simulations. The nodal spacing in the z- and x-
185 directions was 5.0 cm, but at the termination of the macropores the grid was refined to 0.1 with a
186 multiplication factor of 1.5 above, below and adjacent to the macropores. The y-axis node spacing
187 was 0.4 cm which equals the average diameter of the earthworm burrows.

188 Tectonic fractures and earthworm burrows were represented as 2D-planes in the model with a dip of
189 90 degrees and a uniform aperture along the macropore. Water retention characteristics are taken
190 from (Rosenbom et al. 2009).

191 K_{sat} for the 2D-planes was given by $K_{fs} = \frac{\rho g}{12\mu} (2b)^2$ where ρ is the fluid density, g is gravitational
192 acceleration, μ is the dynamic viscosity, $2b$ is the fracture aperture and K_{fs} is the saturated hydraulic
193 conductivity of a single fracture [LT^{-1}], resulting in $K_{fs(fracture)}=0.817$ cm/min and $K_{fs(biopore)}=1307$
194 cm/min.

195 The water table at 1.5 m depth served as the lower boundary as observed in the summer of 2011
196 when the fieldwork took place and was kept constant for the duration of the simulation. There is no
197 flow through the sides of the model.

198 An infiltration flux of 0.25 cm/min was applied to the surface domain for 100 minutes and
199 increased to 0.70 cm/min for the simulations of the heterogeneous and macroporous soil columns.
200 The flux represents the stormwater runoff from a large nearby impervious area diverted to the
201 smaller infiltration unit. A storage height was set to 30 cm for the infiltration flux of 0.25 cm/min
202 and to 70 cm for the infiltration flux of 0.70 cm/min to prevent lateral surface flow.

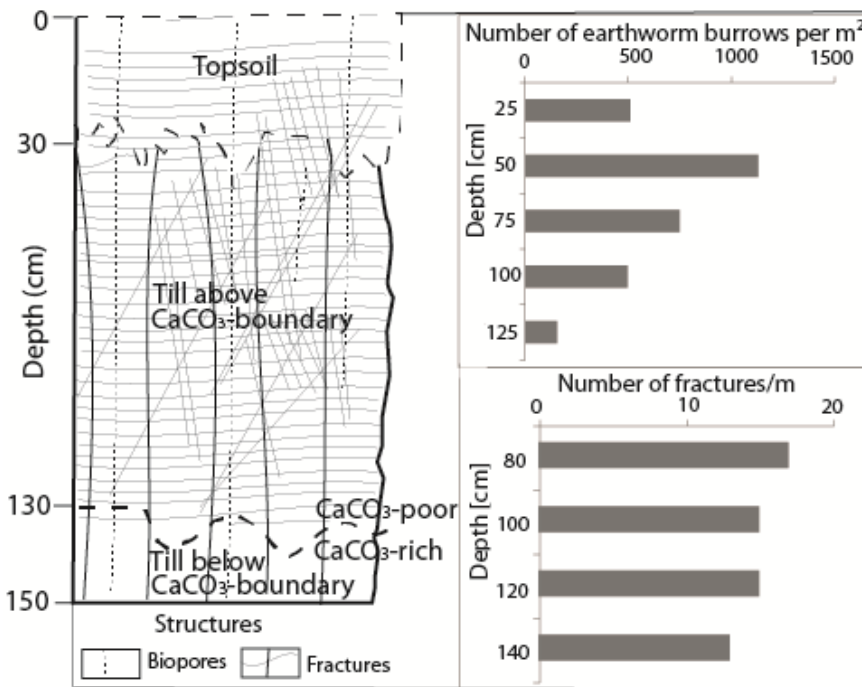
203 The total simulation period varied from 50 hours to 80 days. The initial time step was 10^{-8} min with
204 a maximum time step multiplier of 2.

205

206 **4 Results**

207 **4.1 Tracer test**

208 The results of the field investigations are presented in Figure 3. They include the distribution of
209 hydraulically active earthworm burrows and tectonic fractures across the soil profile and the
210 location of the CaCO₃ at approximately 130 cm depth, with randomly oriented desiccation fractures
211 in the CaCO₃-free soil layer



212
213 Figure 3. Geological log as determined in the excavation including distribution of macropore
214 (vertical tectonic fractures and earthworm burrows).

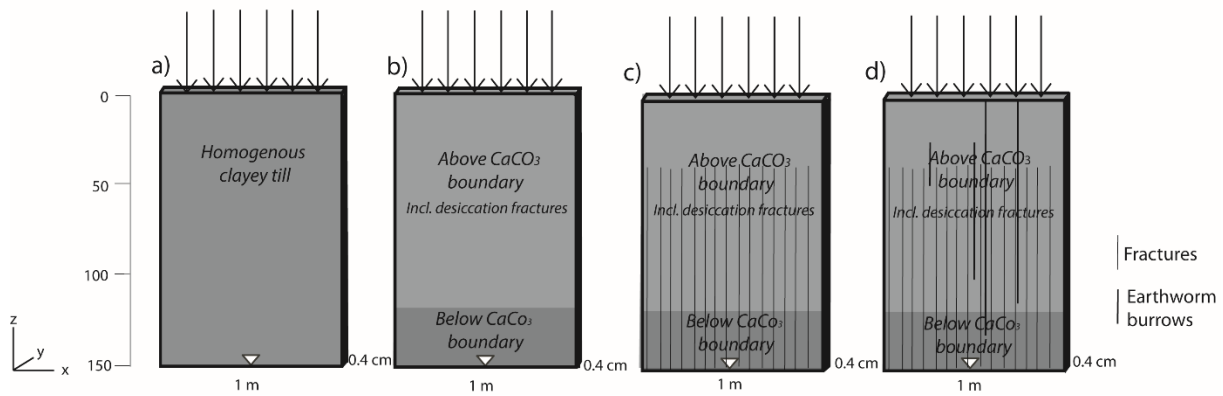
215

216

217 **4.2 Model results**

218 The simplified model scenarios are shown in Figure 4.

219

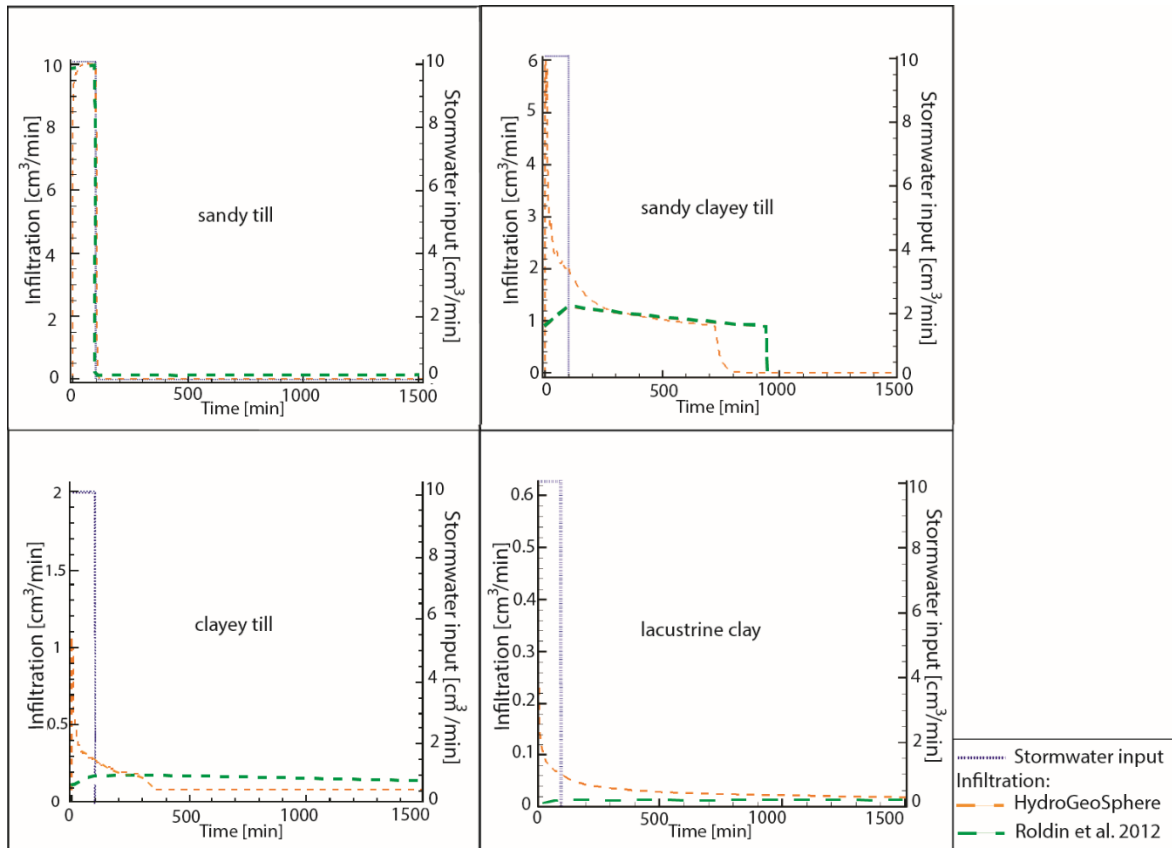


220 Figure 4. Different model domains according to geological description and macropore observations.

221 The weighted mean of K_{sat} for the study area was 0.0648 cm/min, compared to 0.0033 cm/min for
222 the dominant soil type covering the large scale geological map. In this case, an incorporation of
223 detailed knowledge on the sedimentary distribution increases the estimated K_{sat} by a factor of
224 almost 20.

225 The infiltration rates from the HydroGeosSphere and Roldin et al. (2012) models are shown in
226 Figure 5. These rates are of the same order of magnitude, demonstrating that the simple soakaway
227 model gives infiltration rates in homogenous soils similarly to the HydroGeosSphere model.
228 However, there is a significant difference in the initial shape of the hydrograph.

229 Results show the differences within the water balance for the different soil types with clear
230 differences in infiltration behavior over time. Except for the sandy soil, stormwater input exceeds
231 the infiltration capacity and water accumulates on the surface. By examining the area under the
232 curves, the sandy soil can be seen to handle 94% more water than the lacustrine clay.



233

234 Figure 5. Infiltration rates into the four different soil types observed in the study area as simulated
 235 with HydroGeoSphere and the model from Roldin et al. (2012).

236 The soakaway emptying time obtained from the two models is shown in Table 2. The model from
 237 Roldin et al. (2012) approximates the results obtained from HydroGeoSphere within a range of
 238 approximately $\pm 50\%$. This uncertainty is small compared to the uncertainty resulting from different
 239 soil types.

240 Table 2: Emptying times obtained from HydroGeoSphere and the model from Roldin et al. (2012).

	Roldin-model	Roldin-model assuming infiltration only from the soakaway bottom	HydroGeoSphere	Roldin-model/HydroGeoSphere
Sandy till	2 minutes	3 minutes	26 minutes	*
Sandy clayey till	14.1 hours	17.4 hours	12.5 hours	Overestimates 13-39%
Clayey till	4.2 days	5.1 days	8.6 days	Underestimates 51-41%
Lacustrine clay	42 days	52 days	75 days	Underestimates 44-31%

241 * It is not considered relevant to compare emptying time in the scale of minutes

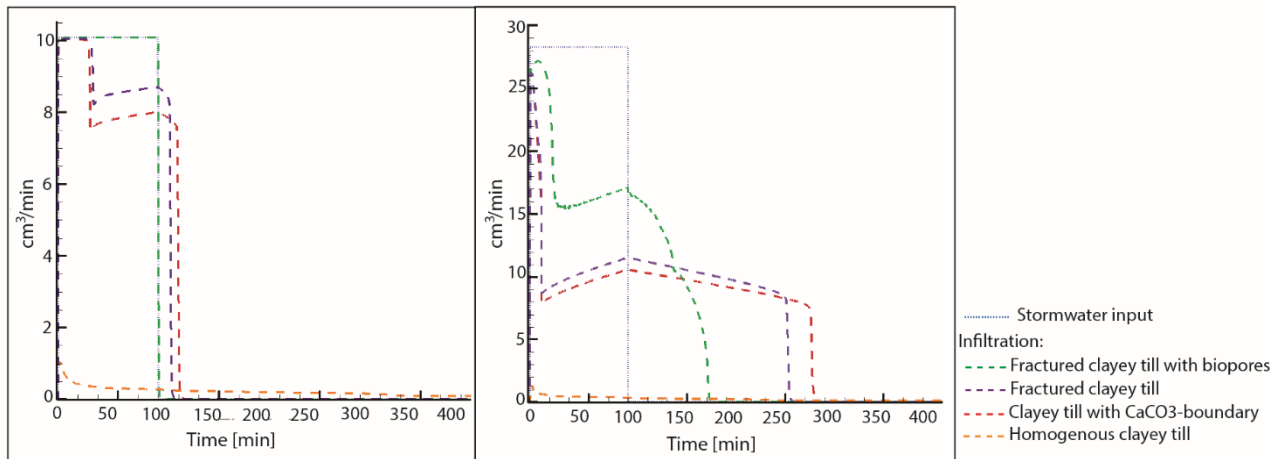
242 Figure 6 displays the infiltration behavior for the heterogeneous clayey till scenarios presented in
 243 Figure 4 for two different stormwater inputs (0.25 cm/min over 100 min and 0.70 cm/min over 100
 244 min).

245 As expected, infiltration capacity is increasing when soil structural features such as macropores are
 246 included. In the first scenario the capacity of biopore infiltration is not surpassed. The effect of
 247 preferential pathways on soakaway emptying times is presented in Table 3. For the second scenario
 248 emptying times vary between 17 days in a homogenous soil and 100 minutes in a soil with CaCO₃-
 249 boundary, fractures and biopores.

250 Table 3. Emptying times obtained from HydroGeoSphere for four different clayey till domains and
 251 two flux-boundary conditions.

	Homogenous clayey till	Clayey till with CaCO ₃ boundary	Fractured clayey till with CaCO ₃ boundary	Fractured and bioporous clayey till with CaCO ₃ boundary
Hydrogeosphere (flux=0.25cm/min over 100 min)	8.6 days	29 minutes	21 minutes	0
Hydrogeosphere (flux=0.70cm/min over 100 min)	17 days	235 minutes	210 minutes	100 minutes

259 At a water inflow rate of 70 cm/min a 22-fold increase in infiltration volume was observed in the
 260 clayey till column when the CaCO₃ boundary and desiccation fractures were included as compared
 261 to the homogenous clayey soil. Infiltration shows a further increase in volume by 8% in a fractured
 262 soil and an increase by another 61% in a fractured soil perforated with earthworm burrows during
 263 the duration of stormwater input.



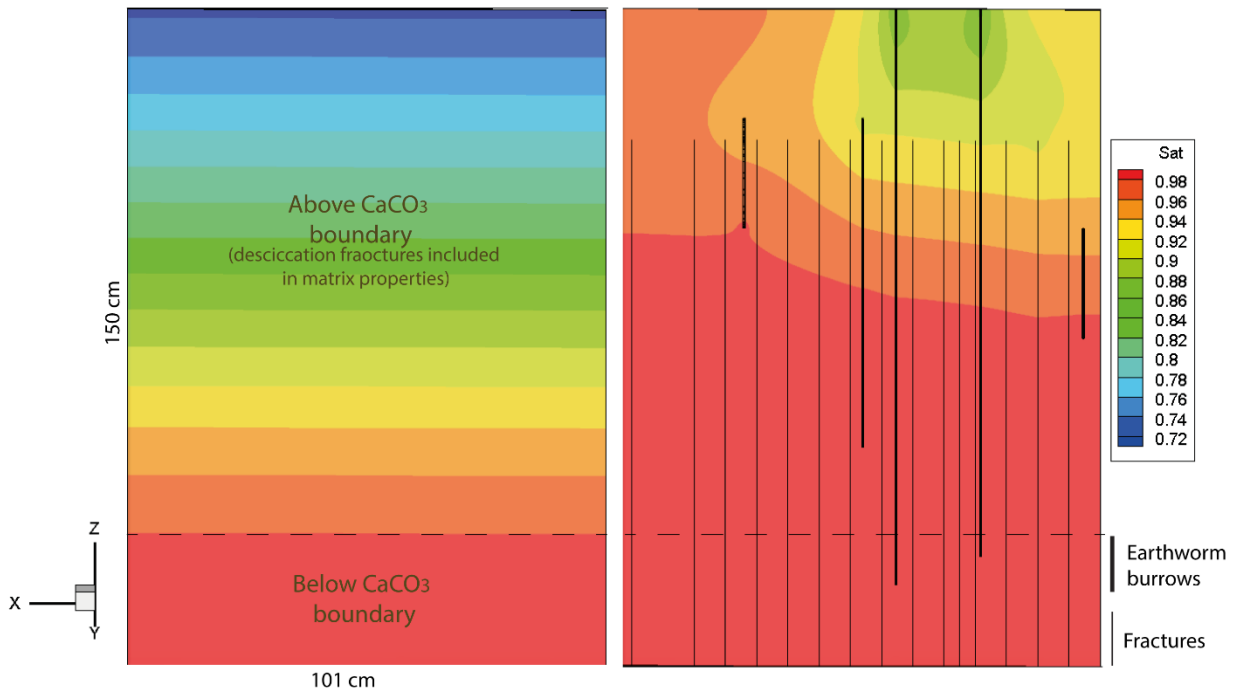
264

265 Figure 6. Infiltration rates for different clayey till domains and two inflow-boundary conditions.

266 Left: Water application rate is 0.25cm/min. Right: Water application rate is 0.70 cm/min (right).

267

268 The importance of earthworm burrows for enhanced infiltration was also shown in the saturation
 269 profiles shortly before and after the rain event (Figure 7). Drainage (decrease in saturation) was
 270 faster along the biopores compared to drainage along the tectonic fractures and in the matrix.



271

272 Figure 7. Saturation profile of clayey till column perforated with macropores before water
273 application (left) and at termination of water application (right). Clayey till column model domain
274 equals outer right column in Figure 5.

275

276 **5 Discussion**

277 *5.1 Differences in model results*

278 Significant differences in the initial shape of the infiltration hydrograph obtained by the Roldin
279 model and HydroGeoSphere model are observed. This is because the model from Roldin et al.
280 (2012) only considers the water level in the soakaway and not the matrix suction in the initially dry
281 soil.

282 *5.2 Model limitations*

283 In these simulations no-flow boundary conditions were chosen on the model sides which may have
284 led to an underestimation of the infiltration rates due to the presence of an artificial flow-barrier. In
285 reality water would also move horizontally through the model boundary.

286 All macropores were represented as vertical 2D planes which might have led to overestimation of
287 infiltration rates due to dominant vertical downward-flow. On the other hand, sub-horizontal freeze-
288 thaw fractures and horizontal earthworm burrows can be interconnected resulting in a network of
289 water pathways which may have led to underestimation of infiltration rates in the model. Studies by
290 Tsakiroglou et al. (2012) document that flow in single fractures is not well represented by single
291 vertical 2D planes but more likely by a 2D channel network.

292 Since this study was based on field observations at small scale with a well-defined geometry of the
293 porous medium and fractures, a discrete fracture approach can best describe the flow conditions
294 (Samardzioska and Popov 2005, Rosenbom et al. 2009). However, at larger scales it is difficult to
295 account for every single fracture because of the computational cost of the simulations. For these
296 cases it can be advantageous to employ a dual porosity approach (Samardzioska and Popov 2005).
297 A dual porosity approach divides the domain into two separate pore systems, the porous matrix and
298 the fractures, with separate hydraulic and transport properties. They interact by exchanging water
299 and solutes in response to pressure head and concentration gradients (Gerke and van Genuchten
300 1993).

301 The simulations did not account for a potential biopore coating. Several studies indicate that walls
302 of earthworm burrows can be lined with a thin hydrophobic mucus layer, secreted by earthworms.
303 When water flows into a biopore, coating along the burrow walls can prevent its movement back
304 into the matrix (Gerke and Kohne 2002, Rosenbom et al. 2009). However, no studies have been
305 carried out yet successfully documenting the influence of biopore-coating on infiltration rates.

306 ***5.3 Risk of contaminant transport through preferential pathways***

307 The simulations focused on the enhanced infiltration of stormwater runoff when macropores are
308 present. However, it should be noted that increased infiltration rates enhance the risk of
309 groundwater degradation by contaminant transport through the same preferential flow routes.
310 Stormwater runoff often carries contaminants such as heavy metals, organic micro-pollutants,
311 nutrients and suspended solids (Butler and Davis 2000). Experimental as well as modelling studies
312 have shown that contaminants can be transported rapidly along fractures (e.g. Hinsby et al. 1996,
313 Jørgensen et al. 1998, Sidle et al. 1998), sometimes even when matrix suction is high (Rosenbom et
314 al. 2009). Infiltration of stormwater runoff should only be considered if either a special treatment
315 facility upstream is installed (e.g. Göbel et al. 2008) or if non- or less polluted roof runoff is
316 infiltrated. Moreover, infiltration devices should only be employed in areas far from aquifers of
317 interest for drinking water supply.

318

319 ***5.4 Improved stormwater management practices in cities and maintenance implications***

320

321 In this study the presence of earthworm burrows decreases the drainage time of the soakaway by
322 110 minutes. Rain gardens or infiltration basins may therefore have greater infiltration rates than
323 subsurface soakaways and should be preferred if space allows. Moreover these systems can filter
324 polluted stormwater runoff through biologically active soils and plants and so remove contaminants
325 from the water (Davis 2007). Rain gardens and infiltration basins should be placed in locations
326 where optimal living conditions for anecic earthworm species (e.g. *Lumbricus terrestris*) can be
327 created, as the worms create deep, mainly vertical burrows for enhanced water flow into deeper soil
328 horizons (Edwards 2004, Lee 1985), thereby improving the soil structure for increased infiltration.
329 Smetak et al. (2011) showed that earthworm population density and diversity increases with age of
330 the urban landscape and with the density of vegetation. Maintaining the soil structure by avoiding

331 tilling of the soil in and around the infiltration based SUD may therefore lead to improved hydraulic
332 performance of the infiltration system over time. The performance of a newly soakaway can be
333 improved by planting and the addition of earthworms to accelerate the process of soil structure
334 development. The resultat bioturbation will increase the hydraulic performance of the raingarden
335 over time and clogging of the system will be reduced.

336 In densely built urban areas, space is often insufficient for the installation of rain gardens which are
337 large enough to handle water from all impervious areas. In such areas a combined design of a small
338 rain garden functioning as a sand trap and water treatment device connected to a subsurface
339 soakaway may be an option. In that way sediment loads into the soakaway will be reduced,
340 preventing clogging of the device and thus prolonging its life expectancy.

341

342 **6 Conclusions**

343 Results of this study have shown that the siting and maintenance of infiltration based SUDS are
344 important in clayey sediments. In this study soakaway emptying times simulated on homogenous soil
345 blocks varied between a few minutes and 75 days. The hydraulic performance of soakaways can be
346 optimized by optimal siting through a detailed geological investigation (Bockhorn et al. 2014).

347 Simple soakaway models such as that of Roldin et al. (2012) were shown to be applicable to
348 simulate infiltration rates and emptying times of soakaways in homogenous sediments. However,
349 the simple soakaway model significantly underestimates infiltration rates in heterogenous (real)
350 soils since they do not account account for preferential flow routes like fractures and macropores.

351 A detailed geological site investigation is needed for accurate prediction of soakaway performance
352 in glacial deposits because of their large geologic heterogeneity. Areas consisting mainly of low
353 permeable clayey sediments might have patches of sandy deposits which are optimal sites for the
354 placement of infiltration based SUDS. Models employing standard soil physical parameters should
355 be used with care as they do not always realistically describe site specific hydrologic properties.

356 In low permeable clayey soils, infiltration capacities are especially sensitive to the presence of small
357 scale soil physical features such as horizontal and vertical fractures, earthworm burrows and
358 structural changes across the soil profile. Upper soil layers typically have increased infiltration
359 capacities, due to the presence of horizontal desiccation fractures above the CaCO₃ boundary and

360 the occurrence of earthworm burrows. Earthworm burrows are most beneficial for infiltration due to
361 their greater aperture compared to fractures and because they often have a direct connection to the
362 surface. Rain gardens may therefore operate with greater infiltration rates than subsurface
363 soakaways and should be preferred if space allows, especially if they are designed so that they
364 provide optimal living conditions for earthworms.

365 **Funding**

366 The work was funded by the Council for Technology and Innovation in Denmark [10-093317]
367

368 **Acknowledgements**

369 The authors wish to thank MSc Daniela Lattner for her help during fieldwork campaigns.
370

371 **References**

- 372 Aquanty Inc. 2013: *Hydrogeosphere Analytics*. Available from: <http://www.aquanty.com/>.
- 373 Backhaus, A. and Fryd, O., 2013. *The Aesthetic Performance of Urban Landscape-Based*
374 *Stormwater Management Systems: A Review of Twenty Projects in Northern Europe*.
375 *Journal of Landscape Architecture*, 8 (2), 52–63.
- 376 Bockhorn, B., Klint, K.E.S, Jensen, M.B., 2014: *Stormwater management: Methods for measuring*
377 *near-surface infiltration capacity in clayey till*. Geological Survey of Denmark and
378 Greenland Bulletin, 31, 47-50.
- 379 Butler, D. and Davies, J.W., 2000. *Urban drainage*. E & FN Spon, London.
- 380 Campisano A., Creaco E., Modica C. 2011. *A simplified approach for the design of infiltration*
381 *trenches*. *Water Science and Technology*, 64 (6), 1362-1367.
- 382 Carsel, R. F. and Parrish, R. S., 1988. *Developing joint probability distributions of soil water*
383 *retention characteristics*. *Water Resources Research*, 24(5), 755–769.
- 384 Creaco E., Franchini M. 2012. *A dimensionless procedure for the design of infiltration trenches*.
385 *Journal American Water Works Association (ISI)*, 104(9), 45-46.

- 386 Davis, A.P., 2007. *Field performance of bioretention: water quality*. Environmental Engineering
387 Science 24, 1048–1064.
- 388 Edwards, C. A., 2004. *Earthworm Ecology* (2nd ed.). Boca Raton, FL, USA: CRC Press.
- 389 Elliott, A. H. and Trowsdale, S. A., 2007. *A review of models for low impact urban stormwater*
390 *drainage*. Environmental Modelling & Software, 22 (3), 394–405.
- 391 Fredericia J., 1990. Saturated hydraulic conductivity of clay tills and the role of fractures. Nord
392 Hydrol, 21, 119–132.
- 393 Freni, G.; Oliveri, E.; & Viviani, G., 2004. *Infiltration facilities design: comparison between*
394 *simplified approaches and detailed physically based modelling*. In: Proceedings of
395 NOVATECH 2004.
- 396 Freni, G., Mannina, G., & Viviani, G., 2009. *Stormwater infiltration trenches: a conceptual*
397 *modelling approach*. Water Science and Technology, 60 (1), 185-99.
- 398 Gerke H.H. and van Genuchten M.T. 1993. *A Dual-Porosity Model for Simulating the Preferential*
399 *Movement of Water and Solutes in Structured Porous Media*. Water Resources Research,
400 29 (2), 305-319.
- 401 Gerke, H. H. and Kohne, J. M., 2002. *Estimating hydraulic properties of soil aggregate skins from*
402 *sorptivity and water retention*. Soil Science Society of America Journal, 66 (1), 26–36.
- 403 Göbel, P., Zimmermann, J., Klinger, C., Stubbe, H., Coldewey, W.G. 2008: *Recommended urban*
404 *storm water infiltration devices for different types of run-off under varying*
405 *hydrogeological conditions*. J. Soils Sediments, 8, 231-238.
- 406 Hansen, A.L., Refsgaard, J.C., Christensen, B.S.B. and Jensen, K.H., 2013. *Importance of Including*
407 *Small-Scale Tile Drain Discharge in the Calibration of a Coupled Groundwater-Surface*
408 *Water Catchment Model*. Water Resources Research 49 (1): 585–603.
- 409 Hinsby K., McKay L.D., Jørgensen P.R., Lenczewski M., Gerba C.P. 1996. *Fracture aperture*
410 *measurements and migration of solutes, and immiscible creosote in a column of clay-rich*
411 *till*. Ground Water 34 (6), 1065–1075.
- 412 Houmark-Nielsen, M., 1999. *A lithostratigraphy of Weichselian glacial and interstadial deposits in*
413 *Denmark*. Bull. Geol. Soc. Denmark, 46 (1), 39–52.

- 414 Hoyer, J., Dickhaut, W., Kronawitter, L. and Weber, B., 2011. *Water Sensitive Urban Design and*
415 *Inspiration for Sustainable Stormwater Management in the City of the Future*, Berlin: Jovis
416 Verlag.
- 417 Jarvis, N. J., 2007. *A review of non-equilibrium water flow and solute transport in soil macropores:*
418 *principles, controlling factors and consequences for water quality*. European Journal of
419 Soil Science, 58 (3), 523–546.
- 420 Jørgensen, P.R., McKay, L.D., Spliid, N.H., 1998. *Evaluation of chloride and pesticide transport in*
421 *a fractured clayey till using large undisturbed columns and numerical modelling*. Water
422 Resources Research 34 (4), 539–553.
- 423 Jørgensen, P.R., M. Hoffmann, J.P. Kistrup, C. Bryde, R. Bossi, and K.G. Villholth. 2002.
424 *Preferential flow and pesticide transport in a clay-rich till: Field, laboratory, and*
425 *modeling analysis*. Water Resour. Res. 38, 1246.
- 426 Klint. K.E.S., 2001. *Fractures in Glacigene Diamict deposits; Origin and Distribution*. Thesis
427 (PhD). Geological Survey of Denmark and Greenland.
- 428 Klint. K.E.S. and Gravesen P., 1999. *Fractures and Biopores in Weichselian Clayey Till Aquitards*
429 *at Flakkebjerg, Denmark*. Nordic Hydrology, 30, 4/5, 267-284.
- 430 Lee, K. E. 1985. *Earthworms: their ecology and relationships with soils and land use*. London:
431 Academic Press.
- 432 Meek, B., Rechel, E., Carter, L. and Detar, W., 1989. *Changes in Infiltration Under Alfalfa as*
433 *Influenced by Time and Wheel Traffic*. Soil Science Society of America Journal, 53(1),
434 238–241.
- 435 Nilson B., Sidle R.C., Klint K.E.S., Bøggild C.E., and Broholm K., 2001. *Mass Transport and*
436 *Scale-dependent Hydraulic Tests in a Heterogeneous Glacial Till - Sand Lens -*
437 *Unconfined Sandy Aquifer System*. Journal of Hydrology, 243, 162-179.
- 438 Roldin, M., Mark, O., Kuczera, G., Mikkelsen, P. S. and Binning, P. J., 2012. *Representing*
439 *soakaways in a physically distributed urban drainage model – Upscaling individual*
440 *allotments to an aggregated scale*. Journal of Hydrology, 414–415, 530–538.
- 441 Roldin, M., Locatelli L., Mark O., Mikkelsen P. S. and Binning P. J., 2013. *A Simplified Model of*
442 *Soakaway Infiltration Interaction with a Shallow Groundwater Table*. *Journal of*
443 *Hydrology*, 497 (0), 165-75.

- 444 Rosenbom, A. E., Therrien, R., Refsgaard, J. C., Jensen, K. H., Ernstsen, V. and Klint, K.E.S.,
445 2009. *Numerical analysis of water and solute transport in variably-saturated fractured*
446 *clayey till*. Journal of Contaminant Hydrology, 104 (1-4), 137–152.
- 447 Sidle R.C., Nilsson B., Hansen M., Fredericia J. (1998). *Spatially varying hydraulic and solute*
448 *transport characteristics of a fracture till determined by field tracer test, Funen,*
449 *Denmark*. Water Resour Res 34(10), 2515–2527.
- 450 Smetak, K.M., Johnson-Maynard, J.L., Lloyd, J.E. (2011). *Earthworm population density and*
451 *diversity in different aged urban systems*. Applied Soil Ecology, 37, 161-168.
- 452 Samardzioska T. and Popov V. 2005. *Numerical comparison of the equivalent continuum, non-*
453 *homogeneous and dual porosity models for flow and transport in fractured porous media*.
454 *Advances in Water Resources* 28, (3), 235-255.
- 455 Therrien R., McLaren R.G., Sudicky E.A. and Panday S.M, (2009). *HydroGeoSphere: A Three-*
456 *dimensional Numerical Model Describing Fully-integrated Subsurface and Surface Flow*
457 *and Solute Transport*. Code documentation and user's guide. Groundwater Simulations
458 Group.
- 459 Tsakiroglou C.D., Klint K.E.S., Nilsson B, Theodoropoulou M.A. and Aggelopolous C.A., 2012.
460 *From aperture characterization to hydraulic properties of fractures*. Geoderma, 181-182,
461 65-77.
- 462 Virahsawmy, H. K., Stewardson, M. J., Vietz, G. and Fletcher, T. D., 2014. *Factors that affect the*
463 *hydraulic performance of raingardens: implications for design and maintenance*. Water
464 Science and Technology: A Journal of the International Association on Water Pollution
465 Research, 69 (5), 982–988.
- 466 Wang, J. S. Y. and Narasimhan, T. N, 1985. *Hydrologic Mechanisms Governing Fluid Flow in a*
467 *Partially Saturated, Fractured, Porous Medium*. Water Resources Research, 21 (12),
468 1861–1874.
- 469 Witherspoon, P. A., Wang, J. S. Y., Iwai, K. and Gale, J. E., 1980. *Validity of Cubic Law for fluid*
470 *flow in a deformable rock fracture*. Water Resources Research, 16 (6), 1016–1024.
- 471 Woods-Ballard, B., Kellagher, R., Martin, P., Jefferies, C., Bray, R. and Shaffer, P., 2007. *The*
472 *SUDS manual (C697)*. CIRIA. Available from:
473 <https://repository.abertay.ac.uk/jspui/handle/10373/994>.

